ELSEVIER

Polymer 43 (2002) 541–553

polymer

www.elsevier.com/locate/polymer

Predicting the binding energy for nylon 6,6/clay nanocomposites by molecular modeling ☆

Genzo Tanaka[a,*], Lloyd A. Goettler[b]

[a]*Solutia Inc., PO Box 97, Gonzalez, FL 32560-0097, USA*
[b]*The University of Akron, Department of Polymer Engineering, Akron, OH 44325-0301, USA*

Abstract

Molecular modeling techniques were applied to predicting binding energies for nanocomposites comprising exfoliated clay layers treated with ammonium salts (usually quaternary) and dispersed in nylon 6,6 resin. For each of 12 selected ammonium ions (quats), a molecular dynamics simulation was performed at 600 K for 100–300 ps with a time step of 0.001 ps on a computer model built from 20 repeating units of nylon 6,6 polymer, six quat molecules and a montmorillonite platelet. Several conformations were selected from the equilibrated time region, energy minimization carried out and binding energies calculated between nylon 6,6 and the clay platelet, between nylon 6,6 and the quat, and between the quat and the platelet. It was found that the binding energy between nylon 6,6 and the clay platelet decreases almost linearly with the volume of adsorbed quat. Consequently, pristine clay yields the highest binding strength to the nylon. Clays partially substituted by long quats were found to be equivalent to those fully substituted with short quats.

Keywords: Binding energy; Molecular modeling; Nanocomposites

1. Introduction

Polymer–clay nanocomposites have emerged as a new class of materials in the last decade of the 20th century. They have superior properties such as higher tensile strength, heat resistance, and are less permeable to gas at a lower level of loading compared with traditional composites [1–11]. Earlier industrial successes of nylon 6 nanocomposites inspired us to design nylon 66 nanocomposites.

In the formation of nylon/clay nanocomposites, platelets initially stacked together to form clay particles are intercalated with polymer, exfoliated and dispersed in the nylon matrix. A single platelet layer is sheetlike, having a thickness of only about 10 Å and $1 \times 1\ \mu m^2$ width [12]. The resulting aspect ratio of about 1000 is a contributing reinforcement factor, since, according to classical theories of filler reinforcement [13], the volume fraction and the aspect ratio are the key parameters governing the mechanical properties of composites. Such theories predict that only several percent of clay by volume (vol%) could double or triple the modulus of layered clay nanocomposites [13]. In fact, commercially viable nylon nanocomposites developed by Toyota Research Laboratories in Japan contained as little as 1.5 vol% of clay [1–6].

In the preparation of layered silicate nanocomposites via melt compounding, refined smectic clay is routinely first treated by exchanging metal cations, usually Na ions, adsorbed on the negatively charged surface of the platelets with onium ions, especially quaternary ammonium salts (quats). The thermodynamics between nylon molecules in the melt and the pristine silicate surface are not sufficiently favorable to expand the clay galleries significantly via intercalation, so the pre-treatment of the clay with quats is required with this system to generate stronger interactions. The larger quats, applied from aqueous alcohol solution in which the clay platelets are colloidally suspended, do, by steric hindrance from their presence in the galleries, force the plates into a larger spacing. However, more importantly, they also alter the thermodynamics of the system by introducing new enthalpic interactions with the polymer molecules, causing a greater degree of intercalation that increases platelet spacing to the point where the platelets become exfoliated, at which point they may disperse individually in the matrix.

Because of the strong role played by thermodynamics, all

☆ This paper was originally submitted to *Computational and Theoretical Polymer Science* and received on 4 October 2000; received in revised form on 18 January 2001; accepted on 18 Janaury 2001. Following the incorporation of *Computational and Theoretical Polymer Science* into *Polymer*, this paper was consequently accepted for publication in *Polymer*.

* Corresponding author.
E-mail address: gmastanaka@msn.com (G. Tanaka).

0032-3861/02/$ - see front matter
PII: S1089-3156(01)00014-9

Table 1
Atomic coordinates for montmorillonite [14]

Serial number	Atom	Partial coordinates		
		x/a	*y/b*	*z/c*
1	M1	0.0	0.0	0.0
2	M2	0.0	0.333	0.0
3	M3	0.0	0.667	0.0
4	T1	0.417	0.329	0.270
5	T2	0.417	0.671	0.270
6	K	0.5	0.0	0.5
7	O1	0.481	0.5	0.320
8	O2	0.172	0.728	0.335
9	O3	0.172	0.272	0.335
10	OH(O4)	0.419	0.0	0.105
11	O5	0.348	0.691	0.110
12	O6	0.348	0.309	0.110

quats are not equally effective. Some quats are effective in opening up the gallery, but they may not be compatible with nylon 6,6, leading to a weak interface. Others may not open up the gallery at all. Therefore, two primary problems remain to be solved regarding quat selection: (1) what chemistries will best exfoliate a clay in the nylon matrix, and (2) which of these quats are most effective in providing a high interfacial strength between the dispersed clay platelets and the nylon matrix.

In this paper we treat the second problem since the first problem involves mass transport and polymer diffusion, whose simulations are impractical at the atomistic level. Our approach is to build a model comprising nylon 6,6, a quat, and a montmorillonite platelet on a computer, equilibrate the system by molecular dynamics and energy minimization, calculate binding energies between all of the components: the nylon 6,6 and the clay platelet, the nylon 6,6 and the quat, and between the quat and the platelet. Binding energies provide guidelines for screening quat molecules to make nylon 66 nanocomposites having a strong interface between dispersed clay platelets and the nylon 66 matrix. Further, we attempt to connect simulation results to toughness. This is unique since none of the published work has predicted toughness for aluminosilicates–organic and inorganic compounds, though there are numerous reports on atomistic simulations of aluminosilicate systems.

2. Methods and procedures

A simplified model assuming all montmorillonite platelets to be at low volume concentration and fully dispersed in the nylon 6,6 matrix so that they do not interact consists of nylon 6,6 molecules interacting with quats and exposed silicate surface on one side of a montmorillonite clay platelet. For simplicity, sodium ions are allowed to occupy the surface adsorption sites on the other side of the platelet. Twelve quats having a wide range in polarity are selected for our study (see Table 2).

2.1. Building a montmorillonite crystal

Montmorillonite is one species of smectic clay occurring in bentonite ore. As with most natural minerals, its chemical structure and atom arrangements are not unique. Yet, they are structurally derived from those of the mineral pyrophyllite by random substitutions of aluminum by magnesium ions [12].

The principal building elements of pyrophyllite are a 2-D array of aluminum–oxygen–hydroxyl octahedra sandwiched between two 2-D arrays of silicon–oxygen tetrahedral, forming a three-layered platelet. The tetrahedral and octahedral sheets are able to share common oxygen atoms because they are similar in symmetry and dimensions. Most minerals in this group consist of such platelets, which are stacked parallel to each other [12].

We built a montmorillonite crystal in the following manner: based on partial coordinates calculated from X-ray diffraction patterns [14], we first built a unit cell of a pyrophyllite crystal and combined 18 unit cells into a basic cell for our simulations. Then, we partially substituted aluminum by magnesium ions to obtain a crystal structure of montmorillonite. The above procedure was done using the Cerius2 molecular modeling package (MSI) on a SGI silicon graphics workstation.

The resulting lattice is monoclinic having a space group of C2/m [12,14]. The unit cell constants are 5.23, 8.94, and 9.2 Å for *a*, *b*, and *c*, and 90, 99, and 90° for alpha, beta, and gamma, respectively. Table 1 lists the partial coordinates for montmorillonite. It should be noted that because of the space group symmetry, data in Table 1 contain a redundancy.

According to Olphen [12], a typical montmorillonite with a cation exchange capacity (CEC) of 70 meq of cations per 100 g of the clay has the following chemical formula:

$$[(Si_{3.88}Al_{0.12})^{IV}(Al_{1.64}Fe^{3}_{0.05}Mg_{0.36})^{VI}O_{10}(OH)_2]_2 - M_{0.67}$$

where M represents a monovalent exchangeable cation, and the superscripts IV and VI refer to tetrahedral and octahedral coordination numbers, respectively.

It is possible to achieve an integer number of atoms if the basic cell consists of 50 unit cells. However, the total number of atoms then becomes more than 1800 for the basic cell alone, which is beyond practical simulation using currently available computer hardware. Simplification can be achieved by neglecting Al in the tetrahedral lattice and Fe in the octahedral lattice. Three unit cells then yield the integer formula $[(Si_{24})^{IV}(Al_{10}Mg_2)^{VI}O_{60}(OH)_{12}] - M_2$.

The edge of the parent cell in the periodic boundary system must be larger than twice that of the non-bonded interaction cutoff (~8.5 Å). Further, we require the cell to be square as closely as possible in order to diminish any directional preference. Thus, our parent cell consists of

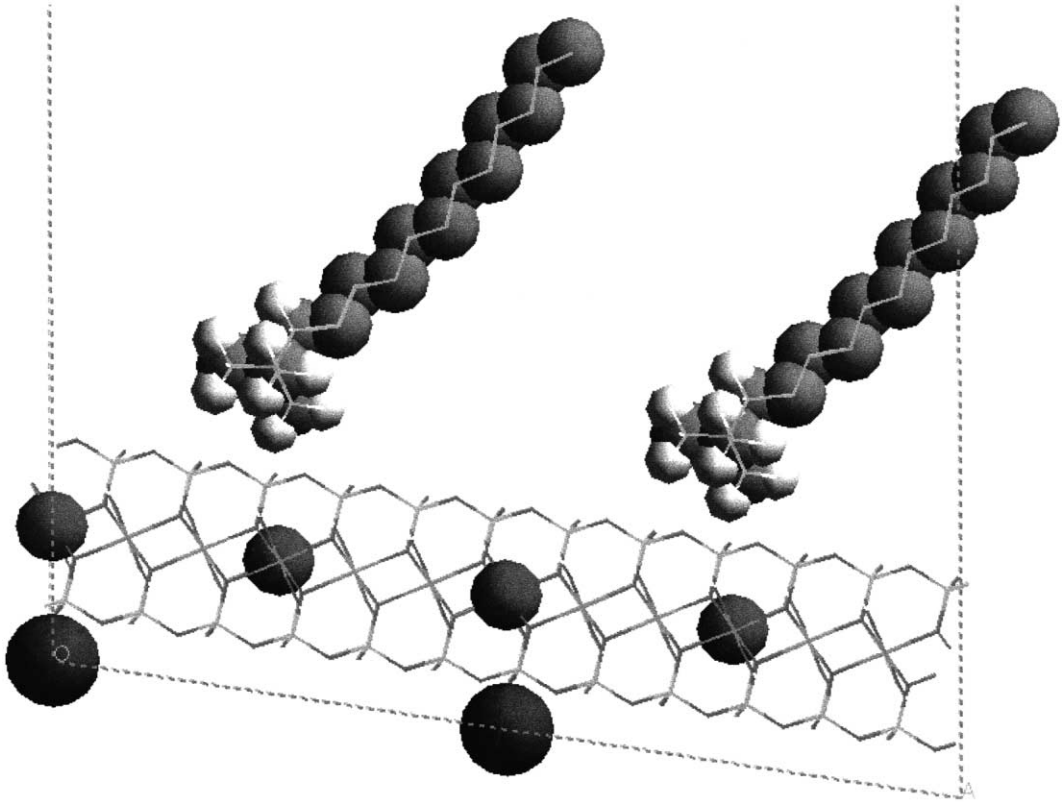

Fig. 1. A clay surface with quaternary ammonium salts $(CH_3)_3NC_{12}H_{25}$. C: grey, H: white. For a montmorillonite crystal, Al and Na are shown by space filled model, and Si and O by the stick model.

$(6 \times 3 \times 1)$ unit cells with dimensions of 31.38, 26.82, and 9.2 Å, respectively. Although the repeating period in the z-axis is nearly the same as the non-bonded cutoff, this repeating period is eventually increased to 125–150 Å to mimic a surface, as described later.

In natural montmorillonite clay minerals, magnesium ions randomly replace aluminum ions in the octahedral lattice. Since an Al ion is trivalent and a Mg ion is divalent, the substitution yields a deficit of positive charge or equivalently an excess of negative charge. This excess of negative charge is compensated by the adsorption of cations on the layer surface, since they are too large to be accommodated in the interior of the platelet [12]. In other words, magnesium ions distribute uniformly in a platelet in a macroscopic sense and cations position themselves on the platelet surface as close to the magnesium ions as possible. Since our parent cell is too small to be a macroscopic cell, we selected the magnesium ion positions in a regular fashion, making their distribution as well as the cation (Na^+) positions just above or below them in the z-axis direction as uniform as possible.

The present study considers only a single platelet. To make the platelet symmetric with respect to cations, half of the 12 adsorption sites of the model, those located on the back side of the layer, were populated with metal (Na) ions, while the other six, located on the side of interest, were filled with a selected quat molecule (Fig. 1).

2.2. Quaternary ammonium salts

Table 2 lists the 10 quats and two amino acids selected for this study. The readily available mono- or di-C18 alkyl quats have been selected as benchmarks because they have been shown experimentally to be moderately effective in enhancing the intercalation of nylon 6,6 molecules, leading to exfoliation and dispersion of the platelets [15]. On the other hand, HTL8, an ethylhexyldimethyl hydrogenated tallow quat treatment, has been found to be more effective in exfoliating and dispersing montmorillonite platelets into a nylon 6,6 matrix [15].

Since nylon 6,6 has high polarity, polar quats would be expected to be more compatible with that polymer, thus enhancing the binding energy to nylon 6,6. This effect could be tested by introducing polar (e.g. carboxyl) groups along the alkyl chain or in the terminal position. Further, amino–enanthic acid was selected to test the different effect imparted by quats versus primary ammoniums, and the effect of chain length in the latter was tested with aminolauric acid. The latter treatment is known to be particularly effective in nylon, since by using it Toyota successfully developed and Ube commercialized nylon 6

Table 2
Chemical formulas, abbreviations, and names of quats and amino acids

Chemical formula	Abbreviation	Name
Pristine	Pristine	
$(H_3C)_3N(C_6H_{13})$	C6	Trimethylhexyl quat
$(H_3C)_3N(C_{12}H_{25})$	C12	Trimethyldodecanyl quat
$(H_3C)_2N(C_{18}H_{37})_2$	2C18	Dimethyldistearyl quat
$(H_3C)_2N(C_{18}H_{37})(C_6H_{11}C_2H_5)$	HTL8	Dimethyl2-ethylhexylstearyl quat
$(H_3C)_2N(C_{18}H_{37})(C_6H_{11}C_2H_5)$	HTL8-50	Dimethyl2-ethylhexylstearyl quat
$(H_3C)_2N(C_{18}H_{37})(C_2H_4OH)$	C18PEO	Dimethylstearylethyleneoxide quat
$(H_3C)_3N(CHOHCH_2)_3H$	PVA3	Trimethylvinyalcoholtrimer quat
$(H_3C)_3N(CHOHCH_2)_6H$	PVA6	Trimethylvinyalcoholhexamer quat
$(H_3C)_3N(CHCOOHCH_2)_3H$	PA3	Trimethylacrylicacidtrimer quat
$(H_3)N(CH_2)_6COOH$	Enanthic	Omega-aminoenanthic acid
$(H_3C)_3N(CH_2)_6COOH$	C7quat	Trimethylomega-aminoenanthic quat
$(H_3)N(CH_2)_{11}COOH$	Lauric	Omega-aminolauric acid

nanocomposites having tensile moduli about 40% higher than the neat polymer [1].

Quats were built using the united atom approximation in which carbon atoms are made to absorb the hydrogens in methyl, methylene, and methine groups, increasing their masses and van der Waals radii. In this way, the number of atoms and likewise the computation time can be reduced by 50–67% for a single quat system. For example, quat $(CH_3)_3NC_{12}H_{25}$ may reduce to $C3_3NC2_{11}C3$, where C3 and C2 represent $-CH_3$ and $-CH_2$ groups in the united atom approximation. The number of atoms reduces to 16 from 60. In some instances, not all $-CH$, $-CH_2$, and $-CH_3$ were reduced to C1, C2, and C3, respectively, in order to test the validity of this approximation.

2.3. Building a system

After a montmorillonite platelet, quat, and nylon 6,6 were built, we constructed our system by substituting six Na ions on one side of the platelet with six quat molecules on the other, as described above, and adding a nylon 6,6 molecule to the platelet–quat complex.

The $N_4—CH_2$ bond of the quat was oriented perpendicularly to the *xy*plane of the montmorillonite [16] and the N_4 atom was placed just above the corresponding Mg position so that the van der Waals radii of the methyl groups and oxygen atoms on the surface of the clay nearly touched but were not overlapped. Their positioning was guided by calculating the non-bonded energy. Fig. 2 displays two C12 quat molecules on the montmorillonite surface along with magnesium and sodium ions, as represented by a space-filled model.

2.4. Force fields

The interactions occurring in a system are described by a potential *E*, which consists of harmonic bond length, harmonic bond angle, 3-fold torsional, inversion, and non-bonded interactions, the last of which can be further subdivided into those due to hydrogen bonding, 6–12 van der Waals interactions and Coulombic electrostatic potentials:

$$E = E\text{bond} + E\text{angle} + E\text{torsion} + E\text{inversion} + E\text{hb} + E\text{vdw} + E\text{elestat} \quad (1)$$

The default force field of Cerius2, Dreiding 2.21 [17], was revised since it does not contain octagonal Al and Mg atoms. We added them to the force field parameter list to make our own force field file. Except for their formal charges, their force field parameters such as van der Waals, bond-stretching, bond bending, torsion, and inversion were set to those of the tetrahedral ones. Although this is a crude approximation, any further refinement is not justified considering the low accuracy of the montmorillonite X-ray data. A further refinement could be done after refined X-ray data become available.

Further, we added quaternary nitrogen 'N_4' to our force field file. The number of the lone pair electrons in 'N_4' was set to zero. All other parameters for 'N_4' are equal to those of 'N_3'.

All other settings were Cerius2 default.

The charges of each atom were assigned by charge equilibration [18]. For a quat molecule, we first set the charges of all atoms to zero and then assigned the positive one to the nitrogen atom, followed by the charge equilibration. The positive charge of one (esu) significantly spread over the entire molecule, leaving the charge of the nitrogen negative. Therefore, we also determined the partial charges by semi-empirical MOPAC using the PM3 Hamiltonian and got the qualitatively same results, though the values of individual partial charges obtained by semi-empirical methods were different from those via charge equilibration. A positive partial charge is not localized on the nitrogen atom, but it is still localized around the nitrogen atom and its substituent groups. For consistency, we used the partial charges calculated by the charge equilibration method. The charge delocalization was an unexpected result for us but has been well known [19] thanks to the reviewer.

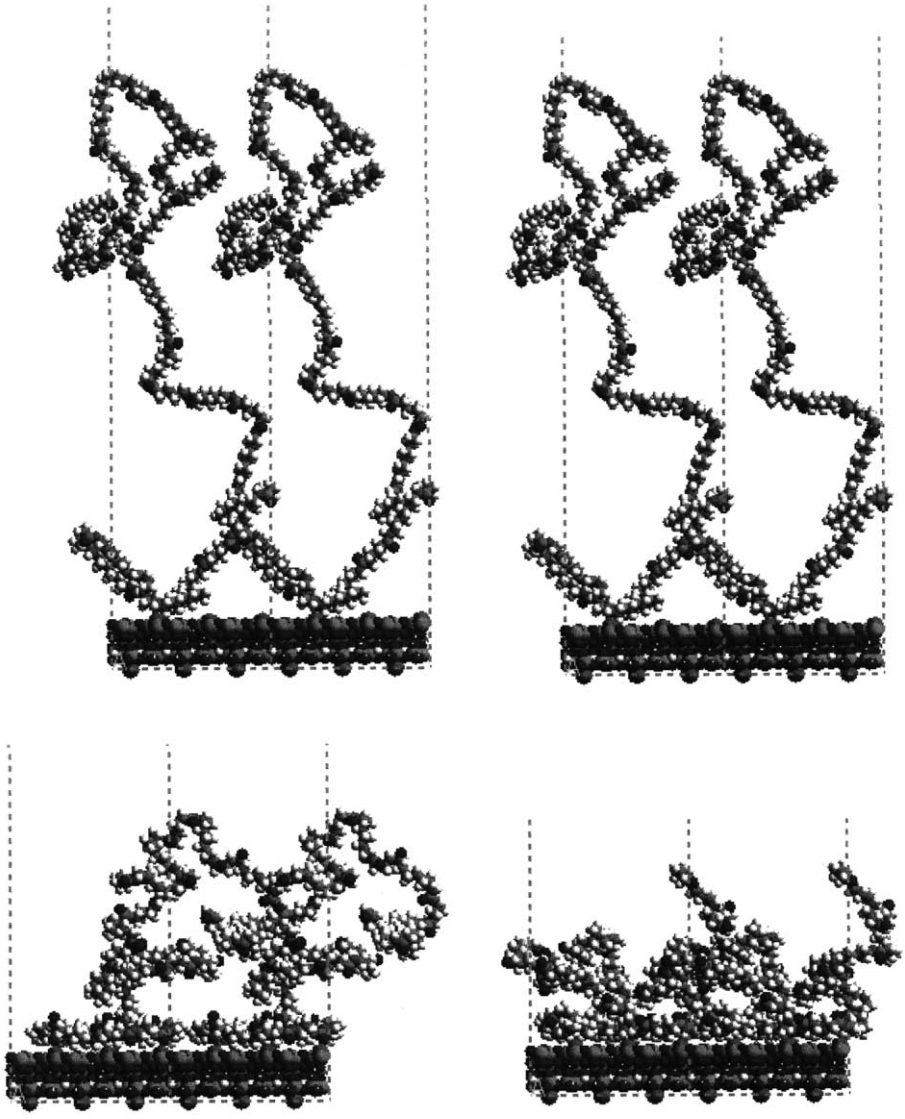

Fig. 2. Four snapshots at 0 (top left), 20 (top right), 50 (bottom left), 100 (bottom right) ps from a trajectory of a 100 ps molecular dynamics simulation at 600 K for a system consisting of a nylon 6,6 chain (20 repeating units) and the montmorillonite surface.

Our usage of the Dreiding force field and the charge equilibrium method is basically the same as Aikin et al. [20]. One difference between the two is the method of handling the long-range interactions. While they used the Ewald summation method, we used a cutoff at 8.5 Å. Either a longer cutoff or the Ewald summation method would be influenced by undesirable effects arising from the residual Na atoms left on the other side of the clay platelet. Although a two-sides model would have been more desirable, in the present work, quats were built on only one side of the clay platelet, leaving Na atoms on the other, in order to limit computation time.

2.5. Nylon single chain

We extracted the conformation at 50 ps (picoseconds) as an initial one from a 200 ps molecular dynamics trajectory for a nylon 6,6 chain of 20 repeating units in vacuum. It spans about 90 Å in the z-direction and 30–40 Å in the x- and y-directions.

2.6. Surface

The lattice constant c of the montmorillonite cell with six quat molecules on one side was extended to 125–150 Å depending on the length of quats and the nylon molecule that was added to it. The closest distance of a part of the nylon to the quat was around 5 Å, so that the nylon chain was attracted to the quat–montmorillonite surface by non-bonded interactions but was far enough away so that its initial conformation hardly affected the equilibrium states of the system. Further, $c = 125$–150 Å assures that the nylon molecule does not interact with the Na-surface of the nearest-neighbor platelet. In other words, even if our

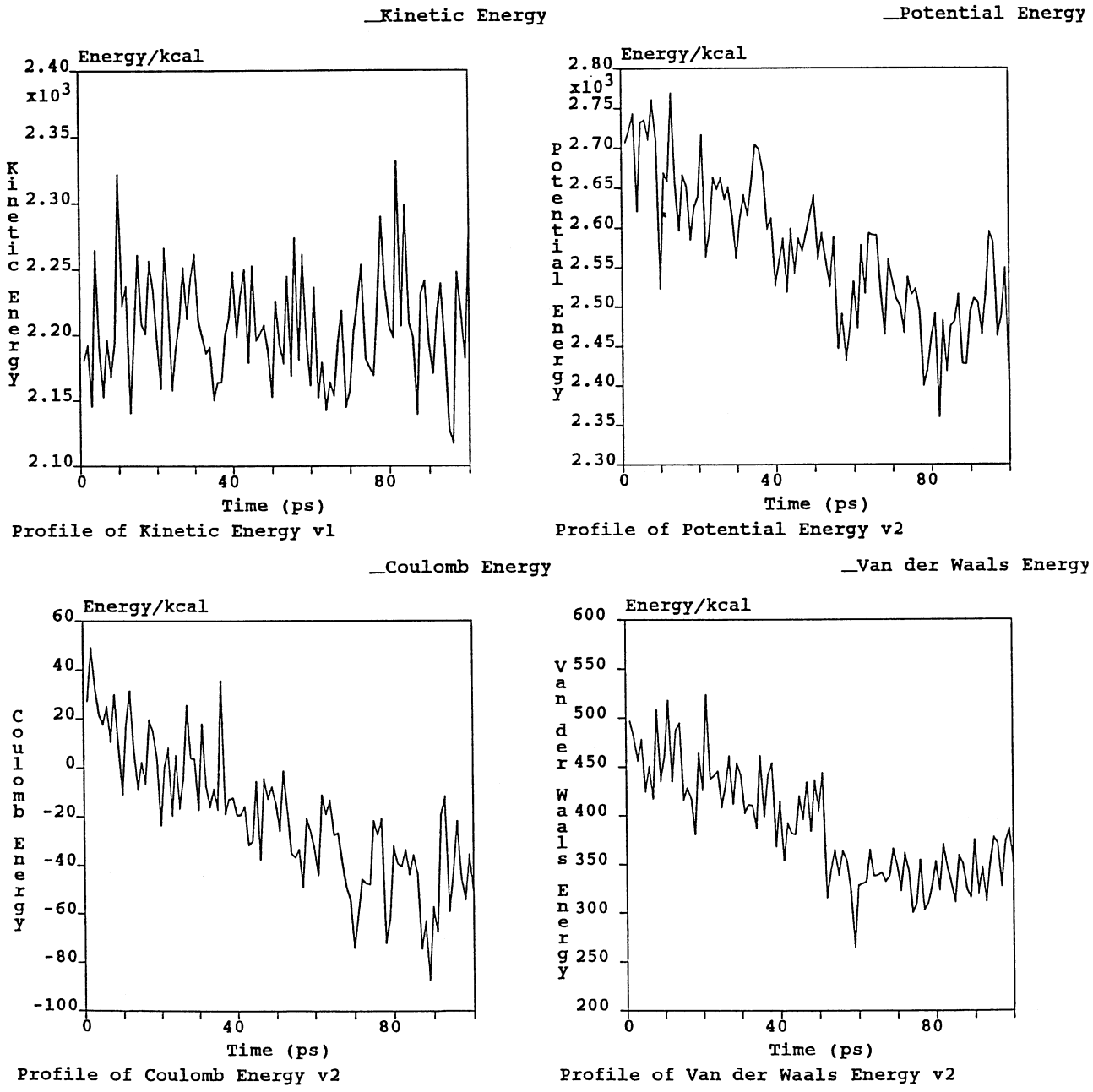

Fig. 3. Profiles of kinetic (top left), potential (top right), electrostatic (bottom left), and van der Waals (bottom right) energies for the simulation shown in Fig. 2.

model is 3-D periodic, there is no interaction between the periodic images in the z direction, creating a pseudo 2-D periodic system [21].

2.7. Molecular dynamics with constraints

Molecular dynamics (MD) simulations were carried out on SGI workstations with a Power Challenger for 100–300 ps at 600 K with a time step of 0.001 ps until the total potential, non-bonded, electrostatic and van der Waals energies became nearly constant for the last 40–100 ps. A high temperature was chosen so that the system could quickly be equilibrated. Since our bond potentials are harmonic, the covalent bonds are stable at 600 K. During the simulations the positions of the montmorillonite and Na atoms were fixed, but the nylon molecule and the quats were allowed to move accordingly.

2.8. Energy minimization

The potential energy of the initial structure was minimized until the root-mean square (RMS) gradient became

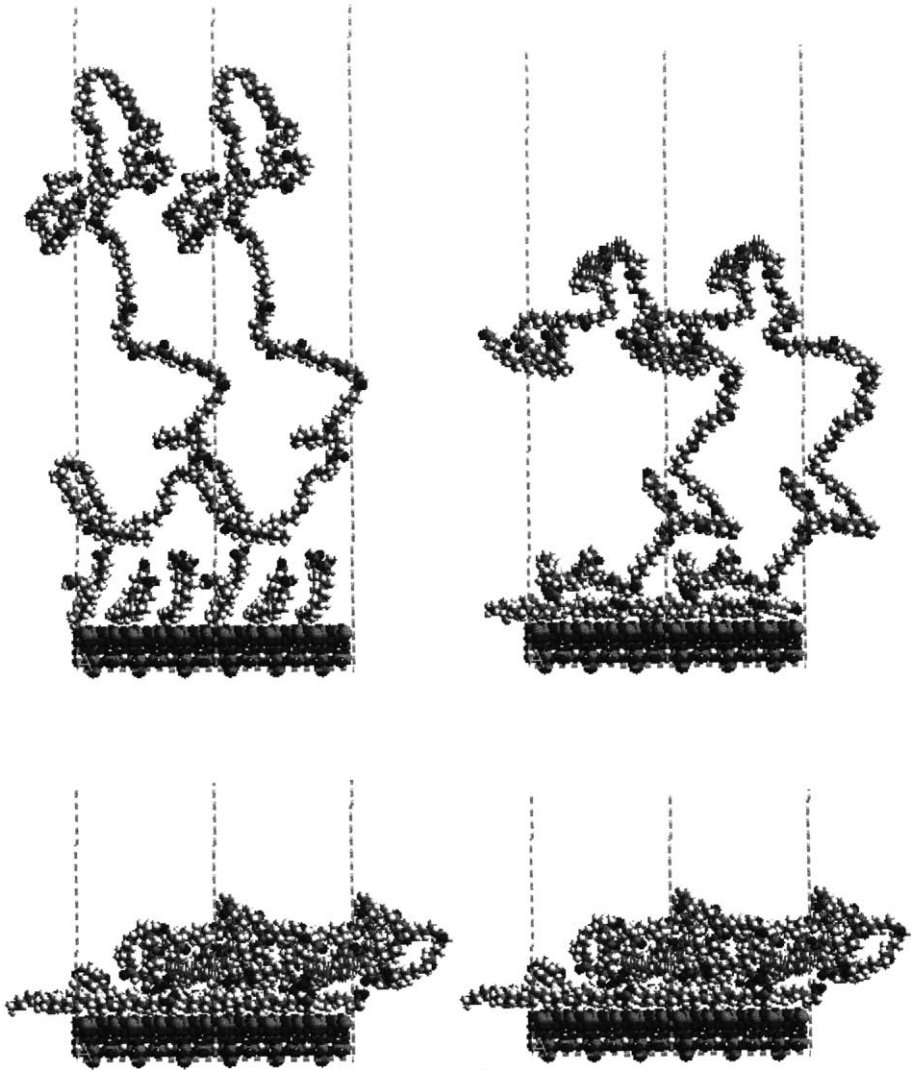

Fig. 4. Four snapshots at 0 (top left), 20 (top right), 50 (bottom left), 200 (bottom right) ps from a trajectory of a 200 ps molecular dynamics simulation at 600 K for a system consisting of a nylon 6,6 chain (20 repeating units), six aminolauric acid molecules [$H_3N(CH_2)_{11}COOH$] and the montmorillonite surface.

0.1 kcal/mol/A. Further, five or six snapshots were extracted from each MD trajectory file during the last 40–100 ps, in which the system became equilibrated and the potential energies were minimized until the RMS gradient became less than 0.01 kcal/mol/A.

2.9. Binding energy

The total potential energy E(nylon,mm,quat) may be written as:

$$E(\text{nylon, mm, quat}) = E\text{nylon} + E\text{quat} + E\text{mm} + E\text{nylon–mm} + E\text{nylon–quat} + E\text{quat–mm} \quad (2)$$

where Enylon, Equat, Emm, Enylon–mm, Enylon–quat, and Equat–mm represent self-energies of nylon, quat and montmorillonite, and interaction energies between nylon and montmorillonite, between nylon and quat, and between quat and montmorillonite, respectively. The self-energies consist of both covalent and non-bonded contributions, and the interaction energies only of non-bonded ones. The binding energy is the negative of the interaction energy.

To calculate the binding energy Enylon–mm, for example, we first created a nylon–montmorillonite system deleting the quat molecules from an energy-minimized conformation and calculated the total energy of the system, E(nylon,mm), without any further minimization). Next, we deleted the montmorillonite platelet and Na ions leaving a nylon 6,6 molecule alone, and calculated the energy of nylon 6,6 molecule, Enylon. Similarly, we deleted the nylon 6,6 molecule from the nylon–montmorillonite system and calculated Emm. Then, the binding energy Enylon–mm may be calculated from the following equation:

$$E\text{nylon–mm} = E\text{nylon} + E\text{mm}–E(\text{nylon, mm}) \quad (3)$$

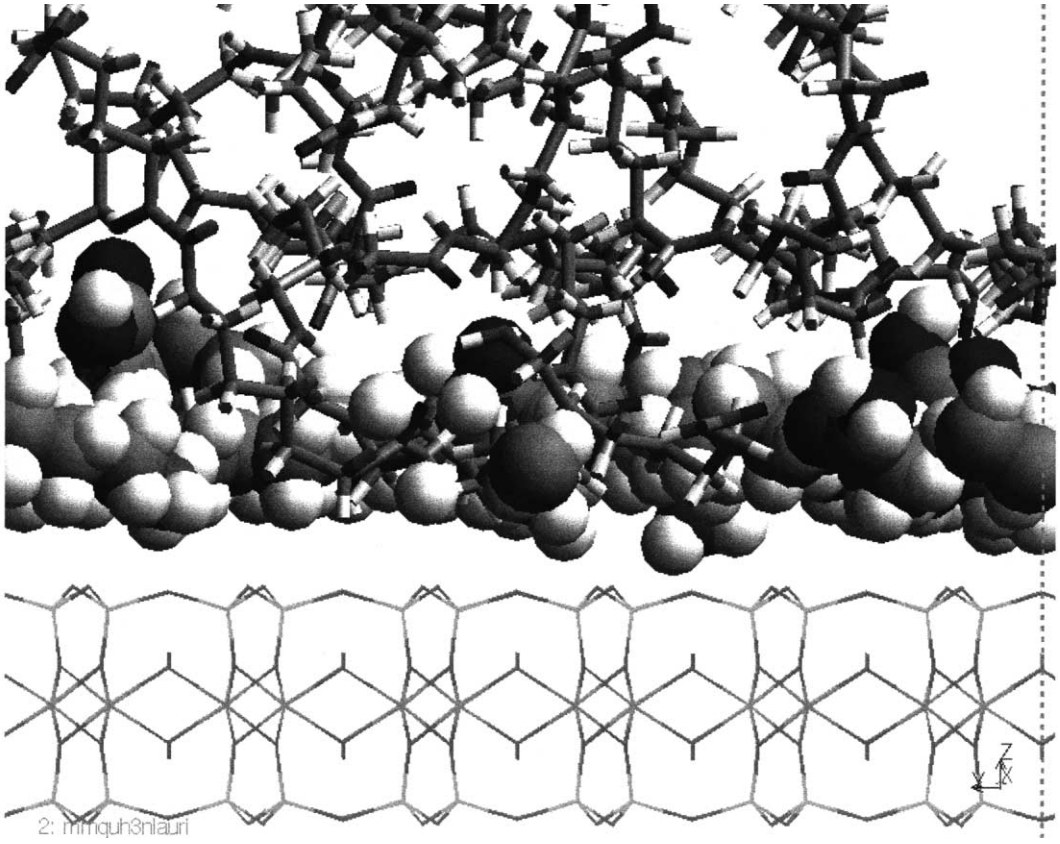

Fig. 5. Close-up of the snapshot at 200 ps in Fig. 4 near the clay surface. Aminolauric acid molecules are shown by space filled model while nylon 66 by cylinder and montmorillonite by stick model.

Similarly, the binding energies *E*nylon–quat and *E*quat–mm are computed as follows:

$$E\text{nylon–quat} = E\text{nylon} + E\text{quat} – E(\text{nylon}, \text{quat}) \quad (4)$$

$$E\text{quat–mm} = E\text{quat} + E\text{mm} – E(\text{quat}, \text{mm}) \quad (5)$$

3. Results and discussion

3.1. Trajectory and equilibrium conformation

In order to demonstrate molecular conformations near the clay surface, four snapshots and energy profiles are shown at 0, 20, 50, and 100 ps in Figs. 2 and 3, respectively, for a MD simulation at 600 K of a nylon 6,6 chain and a pristine montmorillonite platelet. The kinetic energy (upper left in Fig. 3) fluctuates around 2200 kcal/mol throughout the 100 ps period, indicating that the temperature is constant as desired, while the potential energy (upper right in Fig. 3) gradually decreases for the first 60 ps and stays around 2500 kcal/mol for the last 40 ps. The van der Waals energy (bottom right in Fig. 3) decreases until the nylon 6,6 molecule comes close to the surface (see Fig. 2), whereas the Coulombic component more slowly approaches an equilibrium value due to its long-range nature.

Fig. 4 shows similar snapshots at 0, 20, 50 and 200 ps for a nylon 6,6 chain and a montmorillonite platelet exchanged with 6 aminolauric acid ($H_3NC_{11}H_{22}COOH$). Aminolauric acid molecules became flattened on the clay surface within 20 ps elapsed time, and the nylon molecule then docked on top of them within 50 ps. In this case the equilibrium reached in around 50 ps is much faster than for the nylon–pristine clay system shown in Fig. 2. Fig. 5 is a close-up of the 200 ps snapshot in Fig. 4 using a space filling model for aminolauric acid and a cylinder model for nylon 6,6. This figure clearly shows conformations of aminolauric acid molecules and the nylon chain near the clay platelet. Aminolauric acid molecules mostly sit on the clay surface area, so that the nylon 6,6 molecule can occupy only a small portion of it.

Fig. 6 displays conformations of C6 and HTL8 quats as well as lauric acid ammonium ion near the clay surface after the systems were relaxed by energy minimization. The adsorbed ions are not bound to their initial positions above the Mg atoms. They can move around on the surface due to thermal motions (at 600 K). This is particularly so for the smaller ammonium ions, although none have ever been observed to actually leave the surface.

Hydrocarbon chains tend to be straight (*trans* conformation). There are *gauche* conformations, but with a very low probability of occurrence. In HTL8, the stearyl groups lie

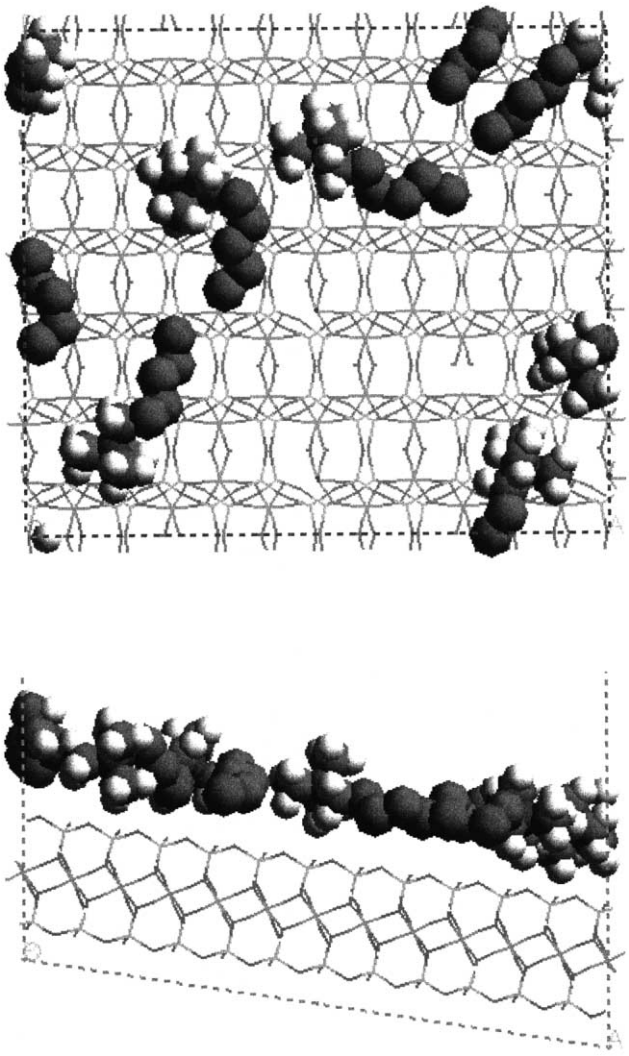

Fig. 6. Top and side views of C6 quats conformations after equilibration.

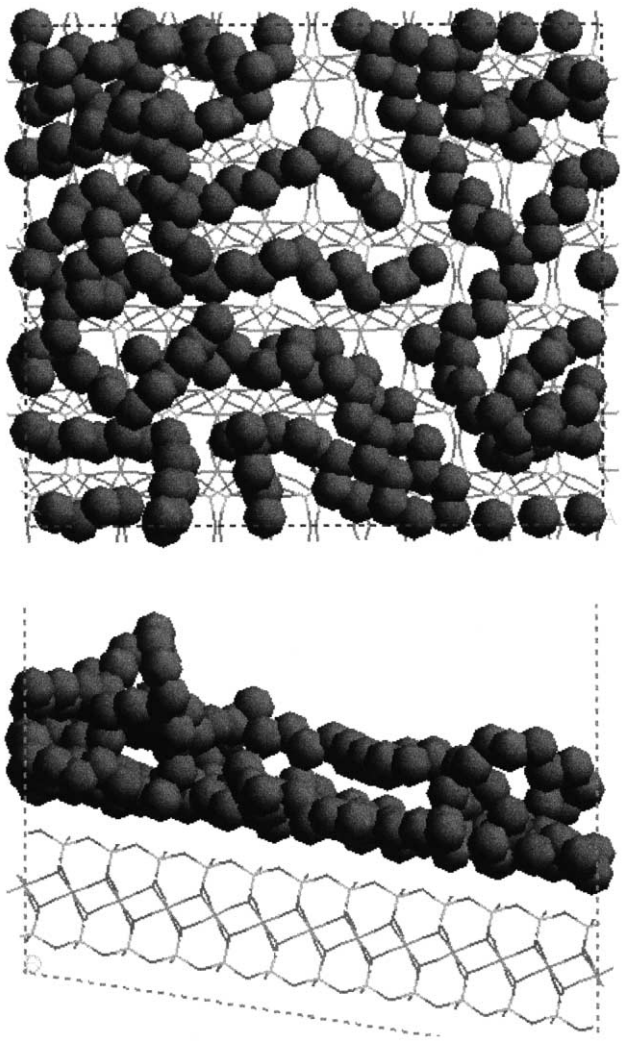

Fig. 7. Quat conformations after equilibration (C18). Top and side views.

down flat and force the ethyl groups to stick outward from the clay surface. This may be preferable for facilitating intercalation, since the steric hindrance of the ethyl groups would prevent the platelets from coming closer together.

As the quat molecules become more voluminous, the nylon molecule collapses less directly on the clay surface and more onto the quats themselves. In other words, the quats shield interactions between nylon and clay, and the larger the quat, the larger the shielding effect. The unexpected adsorption of the hydrocarbon chains of the quats directly onto the silicate layer of the clay surface may be due to electrostatic interactions. A quat molecule has a positive one charge (esu). It spreads all over the quat molecule and does not localize on the nitrogen atom, as mentioned above. All united carbon atoms in the quat molecule are positively charged, while the oxygens on the clay surface are negatively charged. As long as they are separated by more than the sum of their van der Waals radii, interactions between oxygen and carbon atoms are always attractive, mainly electrostatic and secondarily van der Waals.

Since a typical value of surface area per quat molecule is about 140 $Å^2$, all quat molecules cannot lie flat on the clay surface as the volume of the quat molecule increases. Some are up against the clay surface, but others are next to other quat molecules. Consequently, they form a multi-carbon layer. Fig. 7 represents the top and side views of a 2C18 quat, the largest in the present work. It is apparent that the quat layer is much thicker than those in Fig. 6. No quat main chain extends up from the clay surface, except for the ethyl groups in HTL8 as mentioned above and one PVA6 quat molecule to be displayed later.

There arises a question whether or not the initial state affects the final conformation. We performed several simulations in which quat molecules were fixed until an equilibrium was reached during a molecular dynamics run. Once the constraints were removed after that, the quats molecules became flat on the platelet. The resulting conformations were very similar to those reported, although individual atom positions were not identical.

3.2. Binding energy

From the equilibrium conformations we first calculated self and interaction energies, followed by the binding energies between nylon 6,6 and the clay, between nylon 6,6 and the quats, and between the quats and the clay. Tables 3 and 4 summarize these results. Emm values are not included in the above results since they are null due to fixed position constraints. Fig. 8 displays a plot of the binding energy between nylon 6,6 and the clay versus quat volume, whereas Fig. 9 gives nylon 6,6–quat and quat–clay binding energies versus quat volume.

The binding energy *E*nylon–mm between nylon 6,6 and the clay decreases almost linearly with increasing quat volume. A main result of our work is that smaller quats provide stronger interfaces than larger ones, as displayed in Fig. 8. The binding energy *E*nylon–quat slightly increases with quat volume, while *E*quat–mm increases much more sharply.

While HTL8-treated clay, supplied by Southern Clay Products Inc., was experimentally found by transmission-electron microscopy to disperse satisfactorily in nylon 6,6 [22], the resulting tensile strength of its nanocomposites was enhanced only slightly over the neat polymer. Although no definite conclusions can be reached without detailed knowledge of the fracture mechanism(s), the small strengthening effect of the nanoparticles may be attributed in part to a predicted weak binding energy between nylon 6,6 and HTL8-treated clay platelets. *E*nylon–mm for the HTL8 quat is one of the lowest is our study, only about 1/5 ~ 1/6 of that for the aminolauric acid which Toyota used for nylon 6 nanocomposites.

Since quats shield interactions between nylon 6,6 and clay, the combination of pristine clay with nylon 6,6 produces the highest binding energy of all. Thus, nanocomposites produced from untreated clays should be the toughest. In situ polymerization techniques, in which clay is first dispersed in nylon 6,6 monomer without the use of ammonium ion treatment, could potentially lead to superior materials [15].

Quats can be classified by the length of their hydrocarbon chain, which tracks the binding energy, as described above:

Quats	Binding energy (kcal/mol)
C18 or longer	< 30
C12	$100 \sim 150$
C6	$200 \sim 250$

In the present work, all of the initial Na ions adsorbed on the silicate surfaces are generally assumed to be replaced by quats when forming a modified clay. If the Na ions are instead substituted only partially by quats, the above linear relationship would still be expected to hold. However, in this case, the volume of quat used for correlation should no longer be the actual volume of the quat molecule, but an effective volume. For example, if four of six Na ions are replaced by four quat molecules having a volume *V*quat, the proper effective volume would be 2*V*quat/3. If a longer hydrocarbon chain can open up the clay platelet gallery wider, and thus allow nylon molecules to penetrate between the platelets more easily than a shorter one, a smaller fraction of substitution could be used, which would result in a desirably larger binding energy between nylon 6,6 and the clay.

With this in mind, we performed another simulation by replacing only three Na ions out of six with HTL8 quat molecules. The HTL8 molecules on the montmorillonite surface indicates a larger area of the clay surface available for nylon molecule interactions than the fully replaced one. Figs. 8 and 9 also include data points corresponding to this simulation with only 50% cation replacement. The binding energy between nylon and the clay for HTL8-50 increases

Table 3
Equilibrium binding energies for a nylon 6,6 chain and quats near the montmorillonites platelet

Quat[a]	Nylon–clay	Nylon–quat (kcal/mol)[b]	Quat–clay	Volume (A^3)	Surface (A^2)
Pristine	316.0				
$(H_3C)_3N(C_6H_{13})$	232.9	85.4	307.1	156.0	174.1
$(H_3C)_3N(C_{12}H_{25})$	116.0	102.5	403.7	231.4	259.0
$(H_3C)_2N(C_{18}H_{37})_2$	12.7	154.1	507.9	500.6	562.6
$(H_3C)_2N(C_{18}H_{37})(C_6H_{11}C_2H_5)$	20.5	137.5	528.7	380.8	416.1
$(H_3C)_2N(C_{18}H_{37})(C_6H_{11}C_2H_5)$	88.6	111.8	230.5	190.4	208.0
$(H_3C)_2N(C_{18}H_{37})(C_2H_4OH)$	24.4	137.1	568.4	341.1	385.2
$(H_3C)_3N(CHOHCH_2)_3H$	198.9	117.4	380.8	210.7	217.1
$(H_3C)_3N(CHOHCH_2)_6H$	96.7	203.7	442.0	342.1	344.0
$(H_3C)_3N(CHCOOHCH_2)_3H$	161.5	132.7	410.8	287.8	270.7
$(H_3)N(CH_2)_6COOH$	195.5	110.6	365.0	190.0	164.3
$(H_3C)_3N(CH_2)_6COOH$	183.6	96.4	350.0	226.6	210.3
$(H_3)N(CH_2)_{11}COOH$	128.4	119.6	391.2	251.8	280.2

[a] Volume and surface were calculated based on a spherical probe of 1.4 A.
[b] Multiply by 0.413 to convert (kcal/mol) to (erg/cm^2), which is a normal unit for the surface energy.

Table 4
Potential energies at equilibrium for a nylon 6,6 chain and quats near the montmorillonites platelet

Quat	Total	Nylon	Potential energy (kcal/mol)			
			Nylon–clay	Nylon–quat	Quat	Quat–clay
Pristine	173.52	489.52				
$(H_3C)_3N(C_6H_{13})$	−22.37	395.23	162.27	517.77	207.97	−99.22
$(H_3C)_3N(C_{12}H_{25})$	−84.34	385.38	269.41	435.34	152.45	−251.26
$(H_3C)_2N(C_{18}H_{37})_2$	−368.25	385.62	372.90	152.37	−79.12	−587.04
$(H_3C)_2N(C_{18}H_{37})(C_6H_{11}C_2H_5)$	−292.87	361.50	340.91	256.46	32.52	−496.22
$(H_3C)_2N(C_{18}H_{37})(C_6H_{11}C_2H_5)$	−98.48	399.96	201.95	330.10	41.96	−188.60
$(H_3C)_2N(C_{18}H_{37})(C_2H_4OH)$	−152.76	366.53	342.11	440.09	210.73	−357.70
$(H_3C)_3N(CHOHCH_2)_3H$	−149.52	395.79	196.83	430.27	151.95	−228.87
$(H_3C)_3N(CHOHCH_2)_6H$	−344.67	402.21	305.45	194.14	−4.29	−446.36
$(H_3C)_3N(CHCOOHCH_2)_3H$	158.67	394.55	232.95	731.12	469.28	58.42
$(H_3)N(CH_2)_6COOH$	−0.57	375.96	180.45	560.27	294.94	−70.39
$(H_3C)_3N(CH_2)_6COOH$	58.15	418.66	234.97	588.85	266.63	−83.37
$(H_3)N(CH_2)_{11}COOH$	77.22	384.85	256.44	596.96	331.77	−59.50

about 4.5 times compared with that for 100% exchange to HTL8 quats. Since, in Fig. 8, the HTL8-50 point is lower than the expected linear relationship, it appears that our speculation is only qualitatively valid. Giannelis et al. also arrived at a similar conclusion through their thermodynamic approach [23]. The relationship could perhaps be improved by refining the effective volume calculation to include the waters of hydration associated with the Na ions.

It is not clear whether the binding energy between the nylon and the clay alone is sufficient to determine the fracture toughness or the breaking strength. Since the quat molecules adsorb on the clay surface, it may be more reasonable to use the sum of the nylon–clay and nylon–quat binding energies as a better measure of fracture toughness or a surface energy contribution.

Fig. 10 displays the dependence of this sum on quat volume. Since the increase in *E*nylon–quat with volume is more gradual than the decrease in *E*nylon–mm with volume, as shown in Fig. 9, the sum still decreases with increasing quat volume. However, now the difference in the binding energy among different quats becomes smaller. Further, small quats such as C6, PVA3, PVA6, PA3, C7 and enanthic have nearly the same binding energies as pristine clay. One notable result is the PVA6 quat with a —$(CHOHCH_2)_6$ chain. Its *E*nylon–mm is around 100 kcal/mol, but the *E*nylon–quat is the highest of any treatments studied, at 203 kcal/mol. The sum of the two becomes comparable with that of pristine clay. PVA is compatible with nylon 6,6 and in fact one PVA molecule is seen to extend into the nylon 6,6.

3.3. Fracture toughness and interfacial strength

While fracture mechanics has advanced significantly, its application to polymeric materials is still problematical. However, it can be invoked to provide some qualitative interpretations with simple assumptions.

According to Griffith [24], the breaking strength σ_b and elongation at break ϵ_b for a linear elastic homogeneous

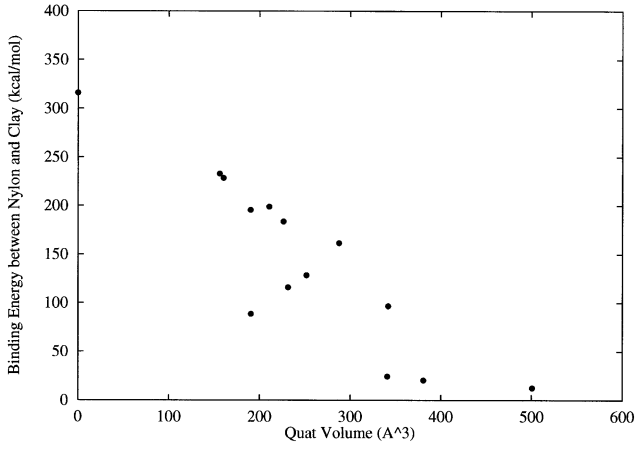

Fig. 8. Binding energy between nylon 6,6 and clay versus quats volume.

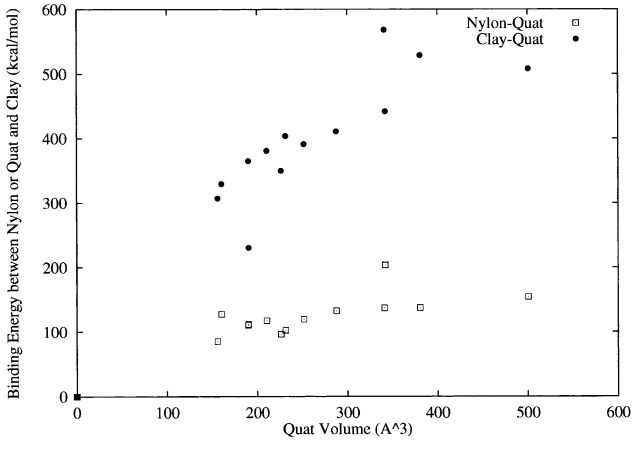

Fig. 9. Binding energies between nylon 6,6 and quat and between quat and clay versus quats volume.

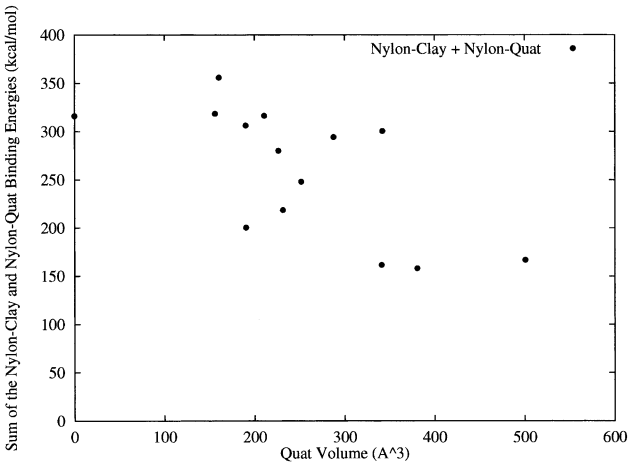

Fig. 10. Sum of binding energies between nylon 6,6 and clay and between nylon 6,6 and quat versus quats volume.

material are given by

$$\sigma_b = (G_c E/\pi l)^{1/2} \quad (6)$$

and

$$\epsilon_b = (G_c/\pi l E)^{1/2} \quad (7)$$

where G_c is the fracture toughness and represents an energy per unit area of crack growth, l the depth of the initial flaw or crack, and E the tensile modulus.

Considering montmorillonite platelets to be fully dispersed in a nylon 6,6 matrix, E would be the same for all quat treatments at the same volume fraction of silicate present. As long as the initial crack length is the same, the breaking strength would be proportional to the square root of the fracture toughness or energy imparted by the clay treatment. In the present analysis, we equate G_c to binding energies predicted above.

If fracture is assumed to initiate at the nylon–clay interface, followed by catastrophic failure of the entire nanocomposite structure, the value of binding energy Enylon–mm could be regarded to represent G_c. Among the systems studied, the HTL8 quat can be taken as a reference since, as mentioned earlier, HTL8-treated montmorillonites disperse well in the nylon matrix. Since Enylon–mm for aminolauric acid-treated clay is about six times larger than that for HTL8 treatment, its breaking strength would be expected on the basis of Eq. (6) to also be higher. It would, furthermore, be higher than the neat nylon 6,6 material, which has an observed breaking strength equal to the HTL8-clay nanocomposite. Similarly, the ratio of the binding energy for pristine clay to that for HTL8 is around 15, so its breaking strength should be higher yet. Thus on considerations of binding energy alone it would be reasonable to expect a doubling of strength via nanoreinforcement.

On the other hand, if a fracture initiates at the interface of both nylon–clay and nylon–quat, it is the sum of Enylon–mm and Enylon–quat that would relate to G_c. According to the binding energies reported in Table 3, the breaking strength improvements for aminolauric acid-treated clay and pristine clay would then be attenuated in comparison with the first case, though still higher than the neat nylon 6,6. C6, PVA3, PVA6, PA3, C7 quat would also yield braking strengths similar to the pristine clay. The binding energy alone would not probably project a two-fold strength increase for this type of fracture without also considering a significant increase in the elastic modulus through the clay reinforcement. Such a stiffening effect is indeed expected, though it unfortunately results in a simultaneous reduction of the elongation at break versus that of nylon 6,6 (see Eq. (7)).

Fracture toughness and interfacial strength also depend on the crystal size of nylon 66, nonhomogeneous stresses and relative orientations of the clay platelets. Crystal sizes could be decreased by a nucleating agent to improve mechanical properties. Fillers like glass fibers have also been used for this purpose. However, none of them has improved toughness and strength as much as that found in nylon–clay nanocomposites. Thus, the crystallite size and nonhomogeneous stresses produced by large fillers may be of secondary importance.

The large aspect ratio of the platelet makes the platelets align parallel like nematic liquid crystals. The spacing between them would be of the order of 100 nm, assuming uniform dispersion. Thus, our simulation corresponds to the dilute limit. Effects of relative orientation are beyond the scope of the present study.

3.4. Platelet spacing

As the snapshots in Figs. 6 and 7 show, the quats lie flat on the clay surface in their equilibrium states. Quat layers are around 4, 6, and 7.5 Å thick for C6, C12, and C18 quats, respectively. These are regarded as the minimum thicknesses that individual quats take up on the single clay surface. If quats with flat conformations intercalate two clay platelets, the gallery distance would be higher at 12, 16, and 19 Å for the above three quats, respectively, since the clay surface and the position of the nitrogen atom in the quat are about 2 Å apart. Since the quats are miscible with themselves, quats on the surfaces of both platelets could mix and assume other conformations than flat ones. Thus, the above estimation should be considered as the minimum inter-platelet spacing that each quat can induce.

According to hydration experiments, the montmorillonite clay has stable states at inter-platelet spacings of 9.7, 12.0, 15.5, and 18–19 Å [25–27]. Although these values are close to those obtained above for C6, C12, and 2C18 quats, the relation between the two is unclear at this moment. It is not clear whether such stable spacing exists in quat-treated clay systems and how its magnitude affects the intercalation of nylon 6,6 molecules into the gallery.

4. Conclusions

The binding energy between nylon 6,6 and a clay platelet decreases almost linearly with increasing volume of the adsorbed quat. Quats with short hydrocarbon chains produce higher binding energies than those with longer ones.

The binding energy between the nylon 6,6 and quat components, on the other hand, increases monotonically with the volume of the quat.

The binding energy between a quat and a clay platelet increases, but much more gradually, with the volume of the quat component than that between nylon 6,6 and the quat.

The substitution of polar groups such as —OH and —COOH for hydrogens on the ammonium ions tends to increase higher binding energies with the nylon. However, pristine clay still yields a high interfacial strength between clay and nylon 6,6, assuming that the clay platelets can be completely dispersed in the nylon matrix.

Partial exchange of the charge sites by long quats produces an equivalent binding energy to a full exchange by short quats and may be preferable for the resulting higher nylon–clay binding energy.

Acknowledgements

The authors express their profound gratitude and respect to Professor Wayne L. Mattice. They thank Drs Saikat Joardar and Yiqi Yang for their discussions on nanocomposites, and Dr Scott Leigh of Southern Clay Products Inc. for providing a reference for X-ray data on montmorillonite. G.T. also thanks Drs Deb Hild, Mukesh Bheda, Doris Culberson, Mikhail Rodkin, and Swadesh Samanta for introducing him to this work, and Dr David Davidson for his encouragement during the course of this work.

References

[1] Okada A, Kawasumi M, Kojima Y, Kurauchi T, Kamingaito O. Mater Res Soc Symp Proc 1990;171:45.
[2] Yano K, Usuki A, Okada A, Kurauchi T, Kamingaito O. J Poly Sci Part A Polym Chem 1993;31:2493.
[3] Kojima Y, Usuki A, Kawasumi M, Okada A, Kurauchi T, Kamingaito O. J Polym Sci Part A Polym Chem 1993;31:983.
[4] Usuki A, Kawasumi M, Kojima Y, Okada A, Kurauchi T, Kamingaito OJ. Mater Res 1993;8:1174.
[5] Usuki A, Kojima Y, Kawasumi M, Okada A, Fukushima Y, Kurauchi T, Kamingaito O. J Mater Res 1993;8:1179.
[6] Kojima Y, Usuki A, Kawasumi M, Okada A, Fukushima Y, Kurauchi T, Kamingaito O. J Mater Res 1993;8:1185.
[7] Messersmith PB, Stupp SI. J Mater Res 1992;7:2599.
[8] Vaia RA, Jandt KD, Kramer EJ, Giannelis EP. Macromolecules 1995;28:8080.
[9] Shi H, Lan T, Pinnavaia TJ. Chem Mater 1996;8:1584.
[10] Giannelis EP. Adv Mater 1996;8:29.
[11] LeBaron PC, Wang Z, Pinnavaia TJ. Appl Clay Sci 1999;15:11.
[12] van Olphen H. An introduction of clay colloid chemistry. New York: Interscience Publishers, 1963.
[13] Guth EJ. Appl Phys 1945;16:20.
[14] Tsipursky SI, Drite VA. Clay Miner 1984;19:177.
[15] Goettler LA, Lysek BA, Powell CE. WO 99/41299, 1999.
[16] Theng KG. The chemistry of clay-organic reactions. New York: John Wiley & Sons, 1974.
[17] Mayo SL, Olafson BD, Goddard III WA. J Phys Chem 1990;94:8897.
[18] Rappe AK, Goddard III WA. J Phys Chem 1991;95:3358.
[19] Maes A, Van Leemput L, Cremers A, Uytterhoevenm J. J Colloid Interface Sci 1980;77:14.
[20] Aicken AM, Bell IS, Coveney PV, Jones W. Adv Mater 1997;9:496.
[21] Misra S, Fleming III PD, Mattice WL. J Comp-Aided Mater Des 1995;2:101.
[22] Goettler LA, Joardar SS, Middleton JC, Lysek BA. WO 00/09571, 2000.
[23] Vaia RA, Jandt KD, Kramer EJ, Gineallis EP. Macromolecules 1997;30:7990.
[24] Griffith AA. Phil Trans Roy Soc (London) 1920;A221:163.
[25] Cebula DJ, Thomas RK, Middleton S, Ottewill RH, White JW. Clays Clay Miner 1979;27:39.
[26] Hawkins RK, Egelstaff PA. Clays Clay Miner 1980;28:19.
[27] Cases JM, Berend I, Besson G, Francois M, Uriot JP, Thomas F, Poirier JE. Langmuir 1992;8:2730.